

# Impact of pile-to-cap fixity on the design and behavior of sensitive structures

Isabella Zapata, John Corven, Seung Jae Lee, and David Garber

- This paper describes the finite element modeling of the connection of prestressed concrete piles to a pile cap or footing considering variables such as pile size, pile embedment length, pile cap concrete strength, interface reinforcement, and pile cap geometry to determine how these variables affect pile-to-cap connection fixity.
- Finite element models of four base bridge types considered to be sensitive to pile-to-cap connection fixity were also analyzed to determine the effect of connection fixity on the behavior of the bridge foundations, substructure, and superstructure.
- The results of the connection analyses revealed that axial compression in the piles and pile embedment length have the greatest impact on the performance of the pile-to-cap connection and that relatively shallow pile embedment lengths can transfer significant moments.
- The bridge models showed that the load effects and behavior of some bridge types are greatly affected by the level of fixity of the pile-to-cap connection; therefore designers need a good understanding of the load transfer mechanisms to properly design sensitive structures.

**F**oundations for many bridges consist of driven piles embedded in pile caps or footings whereby axial loads, lateral loads, and moments are transferred from the bridge to underlying soil or bedrock. In the event of an earthquake or vessel impact, piles can also be subjected to large lateral deflections, which can result in high local curvature and moment demands at various locations along the pile length.

Bridge superstructures can transfer axial loads, lateral loads, and moments to the bridge substructure and foundations. The connection between the pile and pile cap or footing affects the way forces are transferred through the bridge. This connection is typically assumed to be either a pinned or fixed connection. Pinned connections allow transfer of axial and lateral forces but no moments, and they permit some rotation to eliminate excessive moment buildup. A fixed connection allows transfer of axial and lateral forces and development of the full moment capacity of the pile. The assumed connection between the pile and pile cap or footing will affect the stresses in the rest of the structure. The fixity of the connection can be developed using a combination of different methods, including providing sufficient embedment length, roughening the surface of the pile, providing spiral reinforcement around the embedded portion of the pile, extending reinforcement or prestressing strands from the end of the pile into the pile cap, and using mechanical shear connectors with supplemental mild steel reinforcement. This study focuses on developing pile-to-cap fixity using pile embedment with and without dowel reinforcement extending from the end of the pile into the pile cap.

*PCI Journal* (ISSN 0887-9672) V. 67, No. 1, January–February 2022.

*PCI Journal* is published bimonthly by the Precast/Prestressed Concrete Institute, 8770 W. Bryn Mawr Ave., Suite 1150, Chicago, IL 60631.

Copyright © 2022, Precast/Prestressed Concrete Institute. The Precast/Prestressed Concrete Institute is not responsible for statements made by authors of papers in *PCI Journal*. Original manuscripts and discussion on published papers are accepted on review in accordance with the Precast/Prestressed Concrete Institute's peer-review process. No payment is offered.

Currently, 24 states specify a required pile embedment length into the cast-in-place footing or pile cap. Three of these states—Florida,<sup>1</sup> Minnesota,<sup>2</sup> and Wisconsin<sup>3</sup>—specify a pile embedment length for pinned connections of 0.5 or 1.0 ft (0.15 or 0.30 m). Six states—Florida,<sup>1</sup> Wisconsin,<sup>3</sup> Colorado,<sup>4</sup> Illinois,<sup>5</sup> New Hampshire,<sup>6</sup> and Oregon<sup>7</sup>—specify a pile embedment length for fixed connections between 1.0 and 4.0 ft (1.2 m), with Colorado<sup>4</sup> and Oregon<sup>7</sup> calculating required pile embedment lengths based on the plastic moment capacity of the pile about the strong axis, concrete compressive strength, and width of the pile. The other 17 states that do specify a required embedment length do not clarify in their specification whether that embedment detail will lead to pinned or fixed connection behavior.

Research<sup>8–12</sup> has shown that even short embedment lengths (equal to or less than half the pile diameter) can achieve significant moment capacity (up to 40% to 60% of the full moment capacity). Investigations<sup>8,9,13</sup> have also found that the full moment capacity can be developed with embedment lengths much shorter than the 4 ft (1.2 m) embedment required by some states, which was established based on work by Issa.<sup>14</sup>

Incorrect design assumptions about the level of fixity between the pile and the pile cap or footing can lead to undesirable behavior of a structure. The disconnect between current design provisions and past research would suggest that many structures may have a different level of actual fixity between piles and pile caps or footings than is assumed. The primary objectives of the work presented in this paper are to improve

our understanding of the pile-to-cap connection and to analyze the impact of this connection on the overall structure, specifically for structures that are considered sensitive to the pile-to-cap connection.

Two types of nonlinear finite element analysis (FEA) software were used to investigate the behavior of the pile-to-cap connection at two different scales. ATENA from Cervenka Consulting was used to investigate the variables affecting the behavior of the connection at the individual member scale, and Midas Civil from Midas Information Technology was used at the entire bridge structure scale to better understand the impact of pile-to-cap fixity assumptions on the design and behavior of four different bridge types that are sensitive to the pile-to-cap connection detail.

## Pile-to-cap connection models

### Boundary conditions and modeling assumptions

The models used to evaluate the pile-to-cap connection behavior consisted of 6 three-dimensional volume components (pile cap, pile, and four plates) as well as one-dimensional (1-D) line components representing the reinforcing steel and prestressing strands in the piles (**Fig. 1**). Interfaces between volume elements with different materials that shared common surfaces were defined as a fixed contact connection.

Three different materials were used in the ATENA FEA software for the analysis:

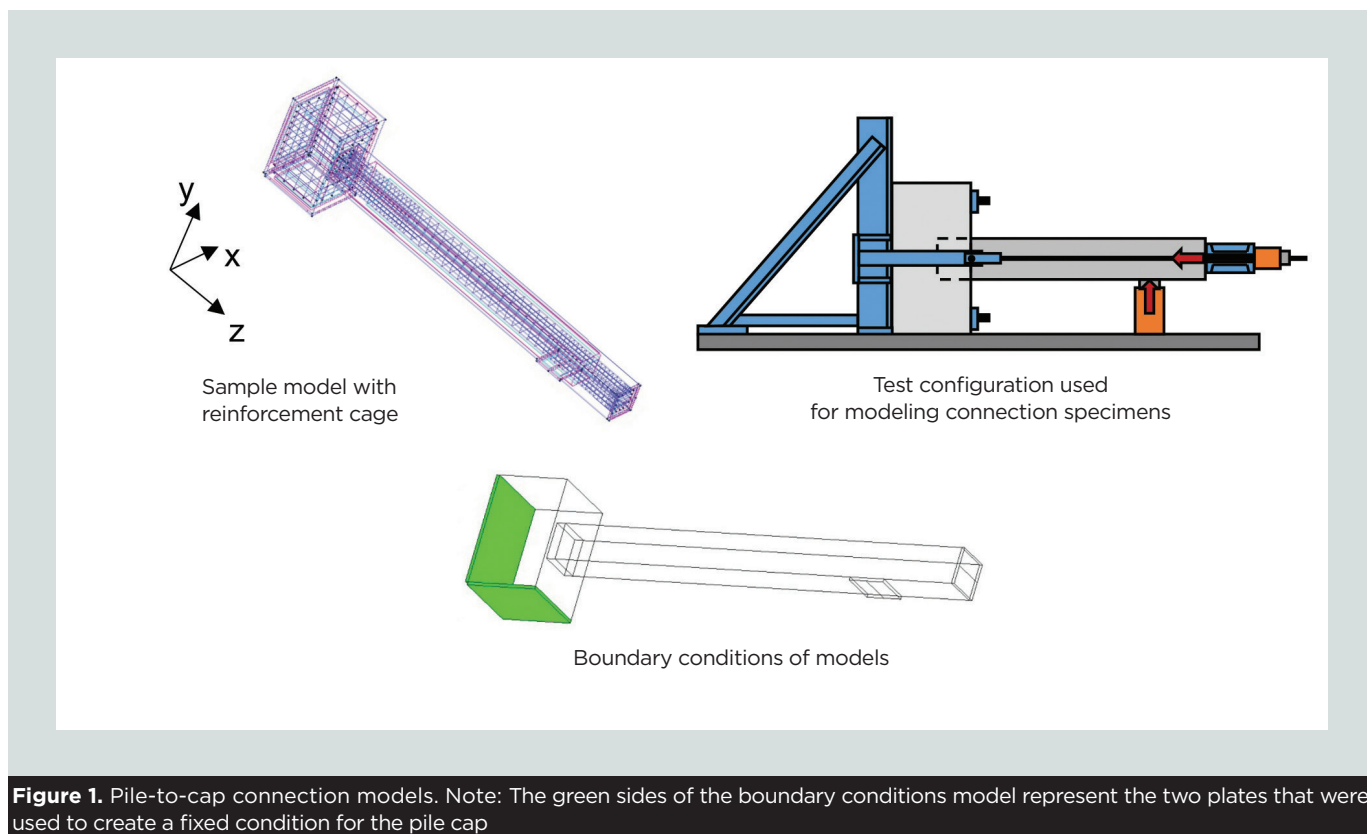


**Figure 1.** Pile-to-cap connection models. Note: The green sides of the boundary conditions model represent the two plates that were used to create a fixed condition for the pile cap

- a solid concrete material for the pile and pile cap
- an elastic solid material for the plates
- 1-D reinforcement material for the reinforcing steel and prestressing strands

Different concrete materials were created for each of the investigated concrete strengths (6000 and 5500 psi [41 and 38 MPa]). The concrete stiffness in the pile cap was temporarily changed to a small value during the prestressing of the pile so that the pile cap did not restrain the pile during the prestressing process. For the steel plates, two different materials, one typical for the steel plates and one with small stiffness, were generated; the latter was used for the steel plates during the prestressing of the piles. The reinforcing steel in the pile cap and the reinforcement confining the strands in the piles were modeled as 1-D reinforcement with a yield strength  $f_y$  of 60 ksi (414 MPa), a yield strain  $\epsilon_y$  of 0.00207, an ultimate strength  $f_u$  of 90 ksi (621 MPa), and a strain at ultimate strength  $\epsilon_u$  of 0.025. Similarly, the prestressing strands were created using 1-D reinforcement but with a tendon-type option. Following are the critical values used for the prestressing strands:

- yield strength  $f_{p1}$  of 204 ksi (1407 MPa)
- yield strain  $\epsilon_{p1}$  of 0.007
- second critical stress  $f_{p2}$  of 243 ksi (1675 MPa)
- second critical strain  $\epsilon_{p2}$  of 0.011
- ultimate strength  $f_{p3}$  of 270 ksi (1861 MPa)
- strain at ultimate strength  $\epsilon_{p3}$  of 0.043

These values were based on the Ramberg-Osgood stress-strain relationship<sup>15</sup> for low-relaxation prestressing strands. The pile-to-cap connection was modeled as a cantilever beam in the horizontal position fixed to a strong floor (Fig. 1). For the models with axial load, an axial load was applied and kept constant throughout the analysis. A lateral load was applied and increased until failure occurred in the specimens; the deflection at the location of the lateral load was measured using a point monitor. Two plates were used to create a fixed condition for the pile cap. A plate with a constraint in the z direction was placed on the back of the pile cap (opposite the pile); a plate with x and y constraints was placed on the bottom of the pile cap (on a face adjacent to the face with the pile) (Fig. 1). These boundary conditions created a moment restraint in the pile cap similar to what would be expected in the laboratory, with the bottom of the pile cap resting on the strong floor and the back fixed to a reaction frame.

A staged construction process was used to properly apply the prestressing force and axial load in the piles before the lateral load was applied to fail the specimens. Three load stages were

used. This process was similar to how the specimens would be loaded in the laboratory and in the field.

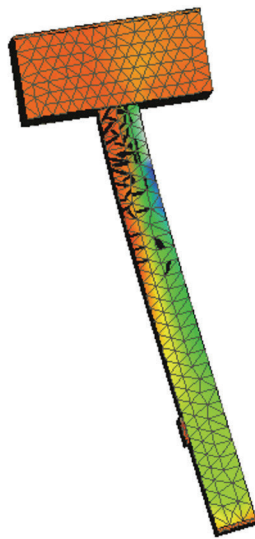
- Load stage 1, prestrain applied to the prestressing strands: The pile concrete strength was defined with typical strength and stiffness associated with the strength at transfer for a prestressed concrete pile. The pile cap concrete was specified with a stiffness close to zero so the pile cap would not restrain the pile during the prestressing process. The total desired prestrain was applied to the pile in 10 steps, locked in, and then kept constant at the end of this load stage.
- Load stage 2, axial load applied to the piles: The desired axial load was applied to the end of the pile in 10 steps and then kept constant on the pile at the end of this load stage. This load stage only applied to systems investigated with axial load.
- Load stage 3, lateral load applied to piles until system failure: An additional small lateral displacement was applied to the pile in 90 steps. The maximum observed load was recorded as the failure load.

This model was validated based on test results from Harries and Petrou.<sup>8</sup> Figure 2 presents a comparison between the estimated failure cracking based on the numerical model and the observed failure cracking based on the test results from Harries and Petrou.<sup>8</sup> Figure 2 also shows a graph plotting the estimated lateral load compared with lateral deflection response, with the reported yield point and maximum measured load indicated. The failure predicted in the numerical model was similar to the failure observed in the experimental testing (Fig. 2). The ultimate capacity was estimated to within 11% of the experimental capacity. Harries and Petrou<sup>8</sup> also reported a lateral load and deformation for the point when the reinforcing steel yielded. This point fell on the curve for the lateral-load-deflection response from the numerical analysis (Fig. 2).

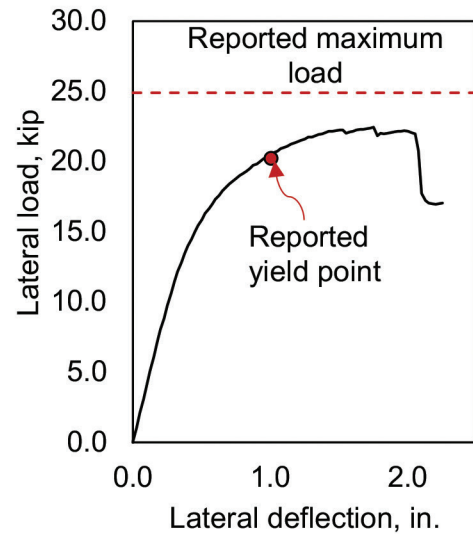
## Member geometry and variables

The primary variables of the pile-to-cap connection modeling were the pile size and the embedment length (Table 1). Three pile sizes were investigated: 18, 24, and 30 in. (460, 610, and 760 mm). The pile details were based on Florida Department of Transportation (FDOT) standard plans for prestressed piles.<sup>16</sup> The distribution of the strands depended on the size of the pile: the 18 in. piles had sixteen 0.5 in. (12.7 mm) diameter Grade 270 (1860 MPa) strands confined with W3.4 (MW22) spiral ties, the 24 in. piles had twenty-four 0.5 in. diameter strands confined with W3.4 spiral ties, and the 30 in. piles had twenty-eight 0.5 in. diameter strands confined with W4 (MW26) spiral ties. A strand pattern with 0.6 in. (15.2 mm) diameter strands with an equivalent prestressing force was also investigated for all pile sizes.

Previously researched embedment lengths primarily varied from 6 to 48 in. (150 to 1200 mm).<sup>8-14</sup> In terms of the



Cracking pattern



Load compared with deflection response.

**Figure 2.** Comparison between numerical model and experimental results from Harries and Petrou (2001). Note: 1 in. = 25.4 mm; 1 kip = 4.448 kN.

pile depth  $d_{pile}$ , these ranges are the equivalent of  $0.33d_{pile}$  to  $2.68d_{pile}$  for 18 in. (460 mm) piles and  $0.25d_{pile}$  to  $2.0d_{pile}$  for 24 in. (610 mm) piles. These research efforts showed that the full moment capacity of the pile could be developed by at least  $1.5d_{pile}$ .<sup>8,9,13</sup> For our study, we selected several embedment lengths between these extreme values to capture how the degree of fixity changes as the embedment length changes. The pile embedment lengths considered in this study were 2 in. (50 mm),  $0.25d_{pile}$ ,  $0.5d_{pile}$ ,  $1.0d_{pile}$ , and  $1.5d_{pile}$ .

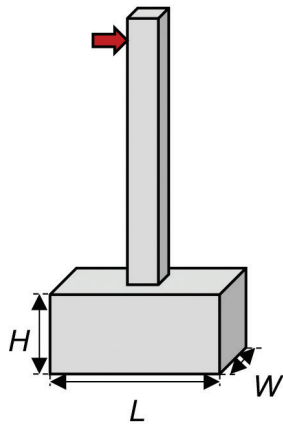
Secondary variables in our study included the pile cap size and the interface reinforcement (**Fig. 3**). Several pile cap sizes were selected to investigate the effect of edge distance on connection strength. The minimum distance between the side of the pile to the nearest edge of the pile cap was based on the American Association of State Highway and Transportation Officials' *AASHTO LRFD Bridge Design Specifications*,<sup>17</sup> and 9 in. (230 mm) was used as a lower limit. **Figure 4** shows the typical reinforcement scheme for the pile cap. Each pile cap was reinforced with no. 6 (19M) reinforcing bars on the side faces, with the bars spaced evenly across the depth of the pile cap, no. 5 (16M) reinforcing bars spaced at 4.5 in. (110 mm) as shear reinforcement, and no. 9 (29M) reinforcing bars in the longitudinal direction spaced at 4.5 in. on center at the location of the pile. The reinforcement detail was based on typical reinforcement used in practice. Interface reinforcement (hooked dowels extending from the ends of the piles into the pile cap) was used with a detail similar to the detail used by Larosche and associates.<sup>18</sup> The primary goal of this reinforcement was to create a positive connection (that is, to allow transfer of axial tension) between the pile and pile cap

**Table 1.** Variables for pile-to-cap connection models.

Parameter	Values investigated
Pile size	18, 24, and 30 in.
Embedment lengths	2 in., $0.25d_{pile}$ , $0.5d_{pile}$ , $1.0d_{pile}$ , $1.5d_{pile}$
Pile strand layout	0.5 and 0.6 in. diameter strand layouts
Axial load	$0.1A_g f'_c$ , $0.2A_g f'_c$ , 0, $-0.1A_g f'_c$ (compression is positive)
Pile concrete strength	Class V (special) (6.0 ksi), Class VI (8.5 ksi)
Pile cap concrete strength	Class II (3.4 ksi), Class IV (5.5 ksi), Class V (6.5 ksi)
Pile cap size	PC1, PC2, PC3, PC4, PC5 (dimensions shown in Fig. 3)
Pile cap reinforcement	With and without confinement reinforcement around embedded pile

Note:  $A_g$  = gross area of concrete pile section;  $d_{pile}$  = depth of pile;  $f'_c$  = 28-day concrete compressive strength. 1 in. = 25.4 mm, 1 ksi = 6.895 MPa.

with minimal moment transfer while allowing for rotation. **Table 1** summarizes the secondary variables that we evaluated, such as axial load, pile and pile cap concrete strength,



Pile cap sizes

( $W \times L \times H$ )

PC1 -  $2.0d_{pile} \times 3.0d_{pile} \times 2.0d_{pile}$

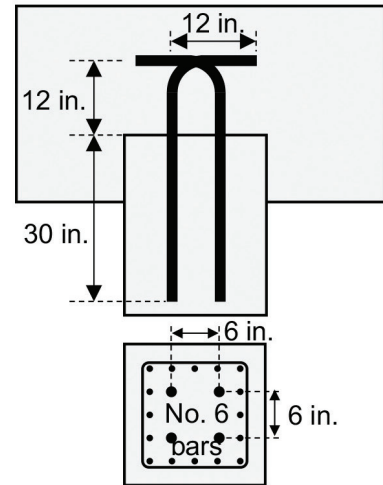
PC2 -  $1.78d_{pile} \times 3.0d_{pile} \times 2.0d_{pile}$

PC3 -  $2.5d_{pile} \times 3.5d_{pile} \times 2.5d_{pile}$

PC4 -  $3.0d_{pile} \times 4.0d_{pile} \times 3.0d_{pile}$

PC5 -  $2.0d_{pile} \times 2.0d_{pile} \times 2.0d_{pile}$

Pile cap sizes



Interface reinforcement detail for pile-to-cap connection models

**Figure 3.** Pile cap sizes and reinforcement details. Note:  $d_{pile}$  = diameter of pile;  $H$  = height of the pile cap specimen;  $L$  = length of the pile cap specimen; PC1 = pile cap specimen 1; PC2 = pile cap specimen 2; PC3 = pile cap specimen 3; PC4 = pile cap specimen 4; PC5 = pile cap specimen 5;  $W$  = width of the pile cap specimen. 1 in. = 25.4 mm; no. 6 = 19M.

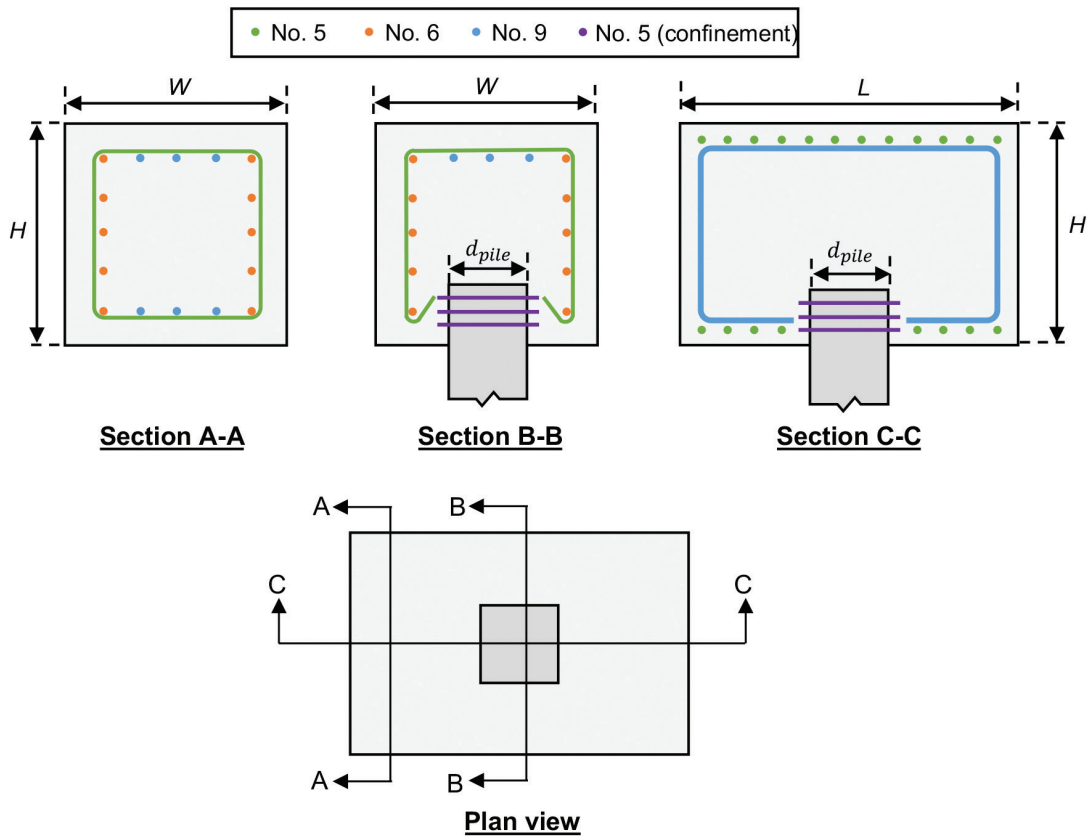


**Figure 4.** Typical reinforcement scheme for pile-to-cap connection models. Note:  $d_{pile}$  = diameter of pile;  $H$  = height of the pile cap specimen;  $L$  = length of the pile cap specimen;  $W$  = width of the pile cap specimen. No. 5 = 16M; no. 6 = 19M; no. 9 = 29M.

and confinement reinforcement (no. 5 [16M] reinforcing bars spaced at 4.0 in. [100 mm]) around the embedded pile.

## Observed failure mechanisms

We used several observed results to determine the failure load and failure mechanism of the connection models. Among the primary results were load compared with deflection response, concrete stress distribution at failure, crack pattern at failure, and maximum stress in prestressing strand at failure. Load and deflection at the load point were measured using monitors at the load points. Stresses and crack patterns were automatically generated during the analyses. Monitors were placed on the prestressing strands to measure the stress in the strands throughout the load application and show the stress in the strand at the ultimate load.

Based on these results, we observed two primary failure mechanisms (Fig. 5). For shallow pile embedment lengths, large amounts of cracking and higher concrete stress were observed in the pile cap between the edge of the pile and edge of the pile cap (Fig. 5). The ultimate strength of the pile-to-cap connection was less than that of the pile itself, and stress in the prestressing strands in the pile did not reach the yield stress in these models. This type of failure was considered a failure of the connection. This connection failure was primarily controlled by the embedment length, which determined the interface length and bearing area between the pile and the pile cap. The failure of the concrete in the pile cap surrounding the pile occurred before any slipping of the prestressing strands was observed, so the strand development length did not control for any of the models.

For deep embedment lengths, large amounts of cracking and higher concrete stress were observed on the tension face of the

pile immediately where the pile extended from the pile cap (Fig. 5). The ultimate strength of the system was equal to the ultimate strength of the pile itself, and stress in the prestressing strands reached the yield stress in these models. This type of failure was considered a failure of the pile. The pile failure occurred when the interface length and bearing area were sufficient to prevent failure of the connection before failure of the pile. The pile failures were controlled by the pile concrete strength and the prestressing strand area and strength.

## Numerical results for pile-to-cap connection models

A total of 131 different pile-to-cap connection models were analyzed. The primary variable investigated through the pile-to-cap connection modeling was the effect of embedment length. Five to eight different embedment lengths were investigated for each of the three pile sizes, with and without interface reinforcement between the pile and the pile cap. The moment response for 18, 24, and 30 in. (460, 610, and 760 mm) piles was normalized based on the estimated pile capacity determined from a layered-section analysis using the University of Toronto's Response-2000 sectional analysis program. Figure 6 shows the response of the system with all three pile sizes, with and without interface reinforcement. There appears to be a linear relationship between embedment length and connection capacity until the capacity of the pile begins to control. A larger portion of the moment capacity was developed in shorter embedment lengths when interface reinforcement was present.

The effect of each secondary variable (axial load in the pile, pile cap concrete strength, pile concrete strength, pile cap dimensions, strand size, and confinement reinforcement) was investigated for one shallow ( $0.25d_{pile}$ ) and one deep ( $1.5d_{pile}$ )

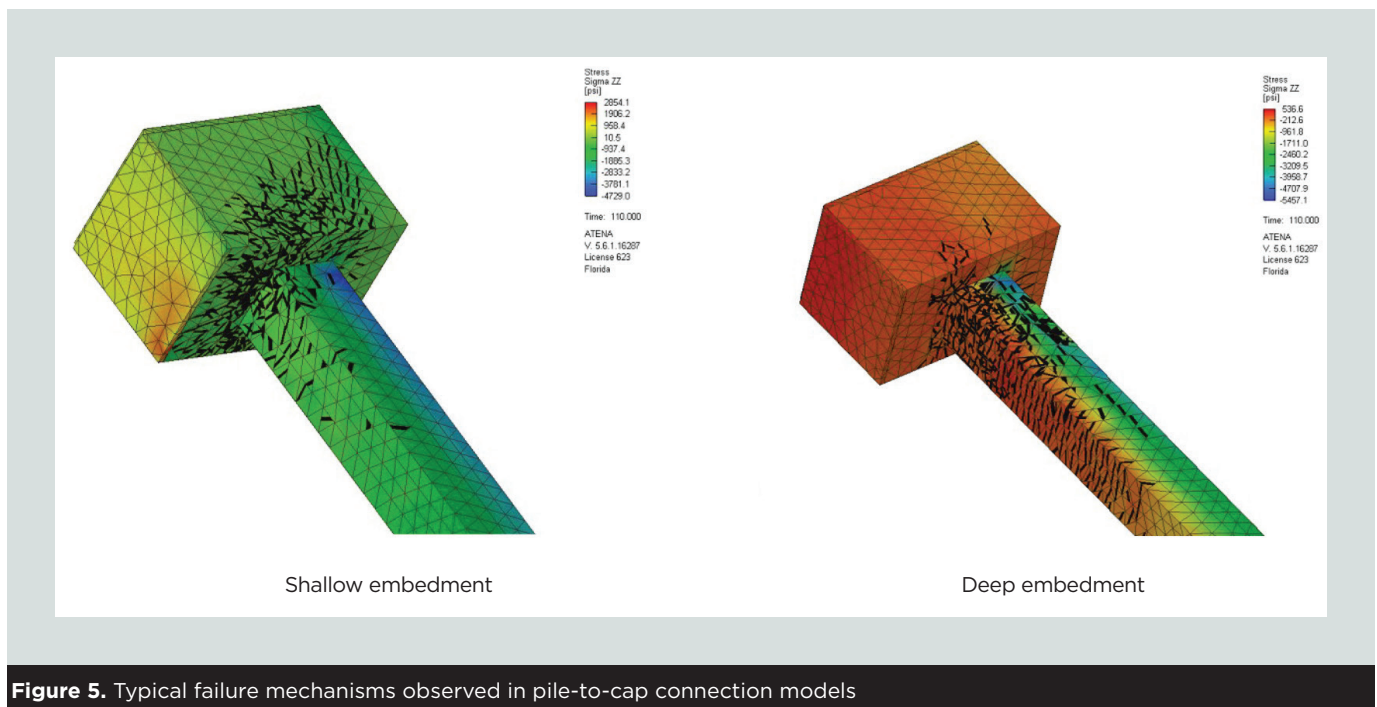
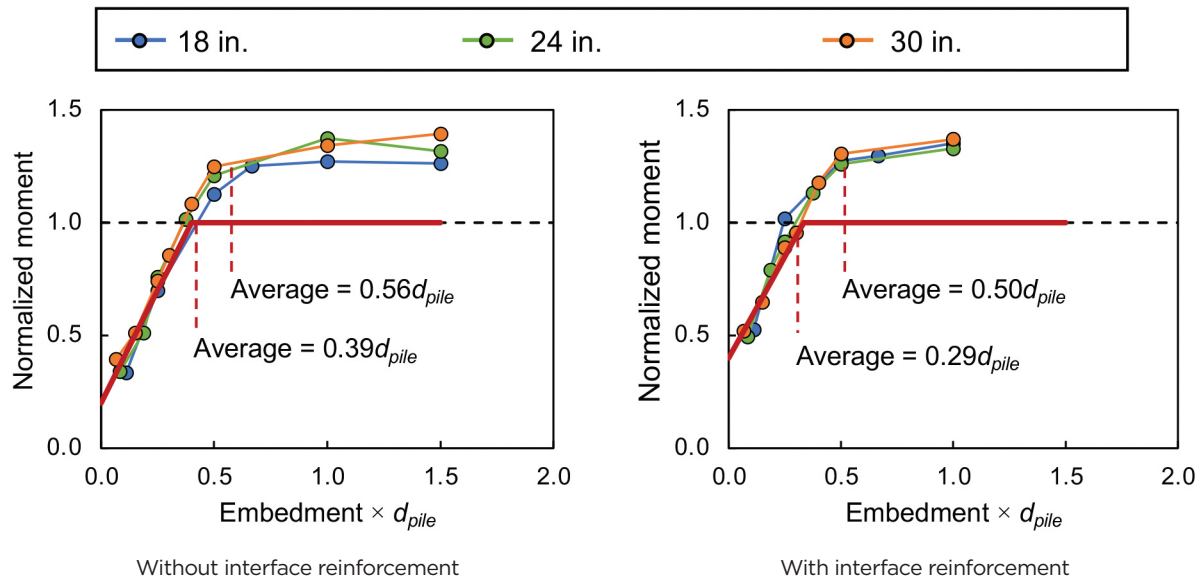


Figure 5. Typical failure mechanisms observed in pile-to-cap connection models



**Figure 6.** Normalized moment compared with embedment length for pile-to-cap connections. Note:  $d_{pile}$  = diameter of pile. 1 in. = 25.4 mm.

embedment. This was done to evaluate the effect of each secondary variable on the connection when the connection controlled the failure and when the flexural strength of the pile controlled the failure. The following effects were observed:

- Axial compression in the pile improved the performance of the connection (**Fig. 7**). Axial load was applied as a function of the gross area of the concrete pile section  $A_g$  and the 28-day concrete compressive strength  $f'_c$ . For shallow embedment, the axial load was found to have the largest impact on the 30 in. (760 mm) piles among all pile sizes, where going from an axial compression load of  $0.1A_g f'_c$  to  $0.2A_g f'_c$  increased the capacity of the system by about 33% (**Fig. 7**). The increase in capacity for 18 and 24 in. (460 and 610 mm) pile systems was about 10%. For the deep embedment, axial load increased the moment capacity of the pile but did not influence the connection performance.
- The pile concrete strength did not affect the behavior of the system when the failure of the system occurred at the connection (that is, for shallow pile embedment lengths). This was because the failure of the connection was due to a failure in the cap. Increasing the strength of concrete in the pile tended to increase the capacity of systems with larger pile embedment. This was because the strength of these systems was controlled by the pile capacity.
- The pile cap concrete strength only affected the strength of the system when the connection failed before the pile (that is, for the shallow embedment) (**Fig. 8**). Because the strength of the system with shallow embedment increased when the pile cap concrete strength increased, the system was likely controlled by the crushing of the pile cap concrete next to the embedded pile. With deep embedment, the strength of the system was unaffected by an increase in pile cap concrete strength because the failure occurred in the pile.
- The size of the pile cap had a limited influence on the behavior of the connection. The capacity of the system with the shallow embedment was only affected by the pile cap size with a  $2d_{pile}$  length. This length corresponded to a  $0.5d_{pile}$  distance between the edge of the pile and the edge of the pile cap, which is similar to the minimum allowable distance in the AASHTO LRFD specifications<sup>17</sup> for 18 in. (460 mm) piles. The pile cap size had no influence on the ultimate strength of the system when failure was controlled by the pile. Confinement reinforcement around the pile did not influence the connection regardless of embedment length. Both observations suggest that the edge distance and reinforcement in the cap were sufficient to confine the embedded pile and prevent splitting of the cap before concrete crushed next to the pile.
- The strand type and pattern had minimal effect on the behavior of the system. In several of the models, a monitor was placed on all of the strands to measure the maximum stress in the strand along the length. The strands were not fully developed for embedment lengths

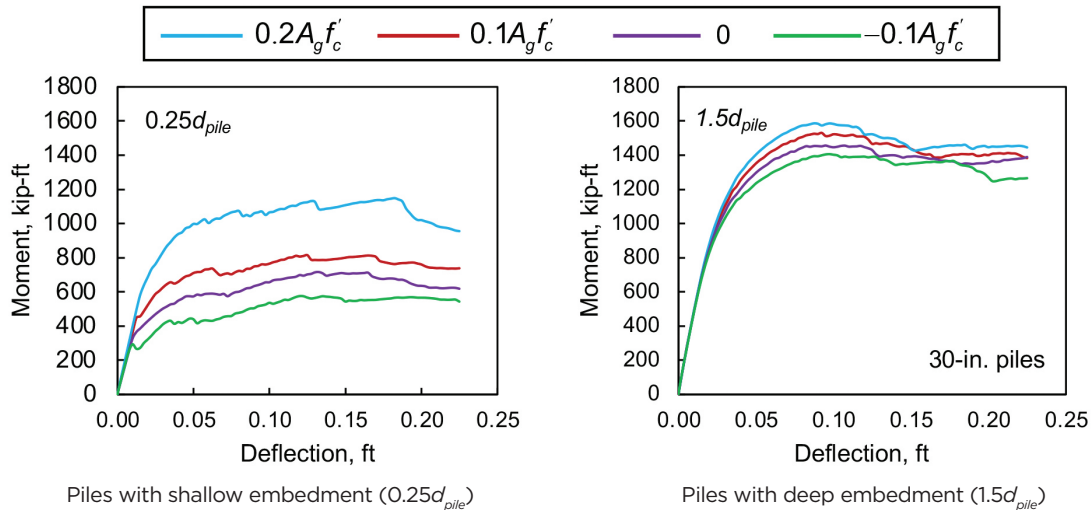


**Figure 7.** Sample moment compared with deflection response for 30 in. piles with varying axial loads. Note:  $A_g$  = gross area of concrete pile section;  $d_{pile}$  = diameter of pile;  $f'_c$  = 28-day concrete compressive strength. 1 in. = 25.4 mm; 1 ft = 0.305 m; 1 kip-ft = 1.356 kN-m.

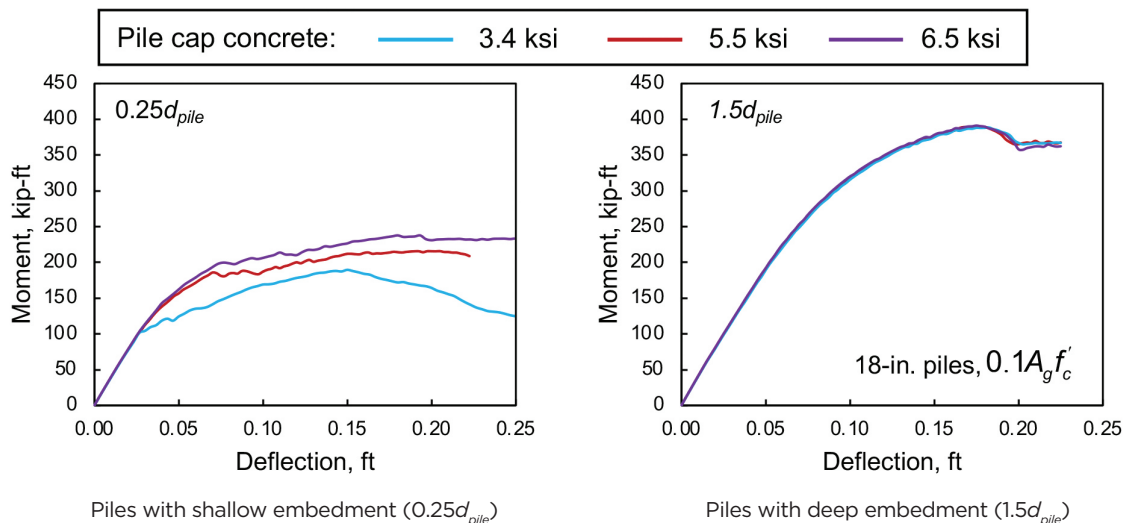


**Figure 8.** Sample moment compared with deflection response for 18 in. piles with axial compression and varying pile cap concrete strengths. Note:  $A_g$  = gross area of concrete pile section;  $d_{pile}$  = diameter of pile;  $f'_c$  = 28-day concrete compressive strength. 1 in. = 25.4 mm; 1 ft = 0.305 m; 1 kip-ft = 1.356 kN-m; 1 ksi = 6.895 MPa.

less than 12 in. (300 mm), which is significantly shorter than the development length required in the AASHTO LRFD specifications.<sup>17</sup> Previous research by Shahawy and Issa<sup>19</sup> suggests that the shorter development lengths observed in our investigation were possibly due to the large compression stresses adjacent to the strands. These stresses were caused by the compression block in the pile bearing against the pile cap as bending of the pile took place. Smaller strand stresses were measured at failure

when crushing of the pile cap concrete next to the pile occurred, suggesting that failure of concrete surrounding the pile occurred before any strand development failures.

In general, pile-to-cap connection behavior is influenced by many different variables and depends on the pile size. The results of the pile-to-cap connection finite element analyses suggest that the current provisions provided by state departments of transportation do not accurately capture the actual

behavior of these connections. An experimental testing program is planned to further investigate the embedment lengths, connection capacity, and strand development in full-size connection specimens and to develop design recommendations for this connection.

### Analysis of structures sensitive to pile-to-cap fixity assumptions

Currently available design provisions may lead to assumptions that connections act as pinned connections when they actually perform like fixed connections. Therefore, this study also investigated how these incorrect design assumptions influence typical designs. Incorrect fixity assumptions have the greatest potential to influence structure behavior if the structure’s design is sensitive to pile-to-cap connection fixity. Fixity assumptions may be critical if one or more of the following three primary conditions that suggest to the engineer that the behavior of a structure is sensitive to the assumed pile-to-cap connection are met:

- when the assumption of the degree of pile fixity can be used to justify or add confidence in substructure stability
- when the structure resists large lateral loads
- when the structure exhibits stiffness-dependent behavior.

We analyzed four base structures (**Fig. 9**) with different pile-fixity levels to investigate the effect of pile fixity on the overall behavior of these bridge types. These structures were selected based on input from bridge engineers with experience in this type of design.

Finite element analyses were performed using Midas Civil to estimate the behavior of these bridges under typical loading conditions with varying levels of fixity between pile and pile cap or footing. Each bridge model included the foundation, substructure, superstructure, springs to represent soil-structure interaction with the driven piles, and boundary conditions. The sectional properties of each element were modeled using the geometry information of each bridge. Materials such as concrete and reinforcing steel were defined with the corresponding properties, and boundary conditions were modeled based on the common practice in bridge engineering.

### Boundary conditions and modeling assumptions

The piles were modeled with general 12-degree-of-freedom beam elements. A pinned connection was assumed at the tip of the pile, and point spring supports were modeled along the length of the embedded pile to simulate the soil-structure interaction (**Fig. 10**). For these models, we selected the typical moduli of subgrade reaction in the x direction  $K_x$  and y direc-

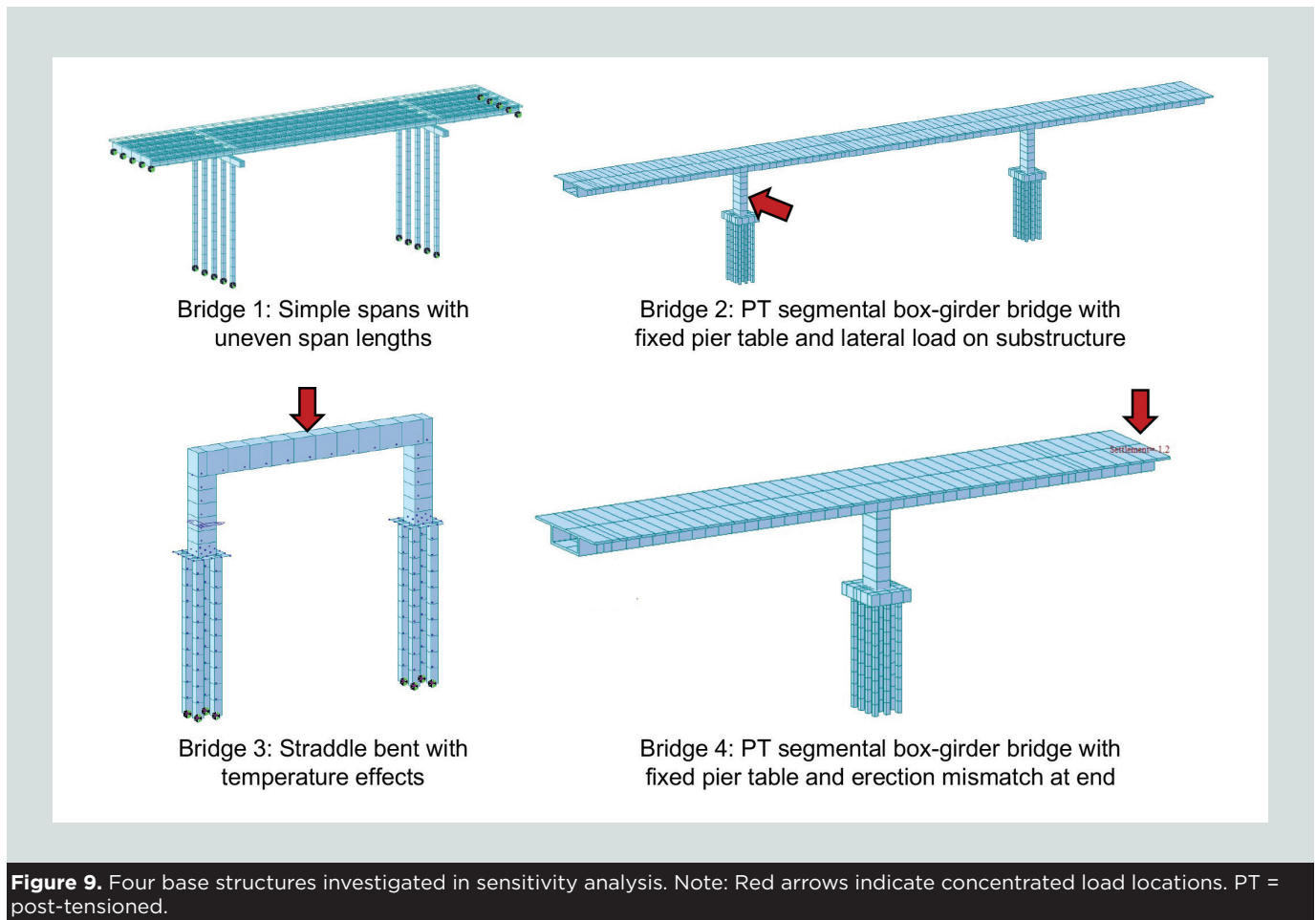


**Figure 9.** Four base structures investigated in sensitivity analysis. Note: Red arrows indicate concentrated load locations. PT = post-tensioned.

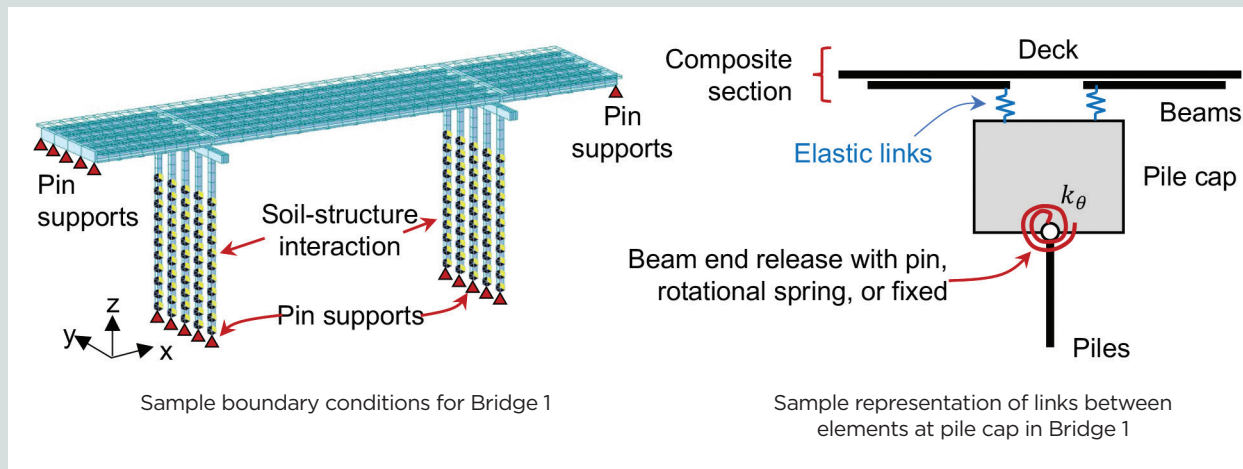


**Figure 10.** Bridge 1 model. Note:  $k_\theta$  = spring rotational stiffness for pile-to-cap connection.

tion  $K_y$  of 0.23 kip/in.<sup>3</sup> (62.4 MPa/m<sup>3</sup>), which corresponds to a dense soil.<sup>20</sup>

The bents were modeled as beam elements and the pile caps as plate elements with section thickness corresponding to the pile cap depth. The bents and piles come into a shared node with the pile cap. The pile-to-cap connection was modeled as fixed or pinned or as a rotational spring, depending on the model (Fig. 10). A beam end release was modeled to the shared node to model a pinned connection. Otherwise, the shared node for the pile-to-cap connection without modification was assumed to be fixed.

A rotational spring was used for bridge 1 because several construction stages of this structure were unstable with the pinned connection. The stiffness of the rotational spring  $k$  was determined from numerical modeling results with different embedment lengths. The rotational stiffness was determined by plotting the moment compared with rotation assuming rigid body kinematic rotation about the pile-to-cap connection. The rotational stiffness was then found based on the slope of the moment-rotation plot in the linear elastic region. As an example, the rotational stiffness  $k$  was 54,610 kip-ft/rad (74,040 kN-m/rad) for a  $0.25d_{pile}$  embedment of an 18 in. (460 mm) pile.

The superstructure, deck elements, beams, and box girders were also modeled with general 12-degree-of-freedom beam elements. Where applicable, pin supports were also used at the end of the superstructure systems (Fig. 10). Beams were modeled as a composite section with the deck.

### Bridge 1: Simple spans with uneven span lengths

**Bridge description** The first structure investigated (Fig. 9) was a simply supported, three-span girder bridge with span lengths of 40, 100, and 40 ft (12.2, 30.5, and 12.2 m). The super-

structure was supported by piles directly embedded in the bent caps. The bearings for down-station and up-station girders were placed on the cap with an offset from the centerline of the cap.

The superstructure consisted of five bulb-tee beams (FIB-45) with an 8 ft (2.4 m) spacing and an 8 in. (200 mm) thick composite concrete deck. Details for the superstructure were designed using FDOT Prestressed Beam v6.0 LRFD design software.

The strand layout for the longer span consisted of thirty-five 0.6 in. (15.2 mm) diameter strands, and twelve 0.6 in. diameter strands were used for each of the shorter spans. The strands were tensioned to 44 kip (196 kN) per strand. The concrete strength of the girders was 6.5 ksi (45 MPa) at transfer and 8 ksi (55 MPa) ultimate.

The standard 18 in. (460 mm) square piles<sup>16</sup> were modeled with 6 ksi (41 MPa) concrete. The number of piles was equal to the number of girders, with the girders located directly over the piles. Piles were directly embedded in the end and interior bents. The typical cross-section dimensions for the end and interior bents were 3.5 ft (1.1 m) wide and 3.0 ft (0.91 m) high, and the concrete strength was 5.5 ksi (38 MPa).

**Construction procedure** Five construction stages were analyzed on bridge 1 (Fig. 11). Construction stages 1 and 2 evaluated the behavior of the structure when the girders were placed in spans 1 and 2, respectively. All girders in a span were placed at the same time for these analyses. The placement of the second-span girders (construction stage 2) caused the maximum moment on the pile-to-cap connection of the support between spans 2 and 3. This construction procedure (with the span 2 girders placed after the span 1 girders) was selected because it resulted in the maximum moment in the connection. The effects of the weight of the concrete deck during construction were analyzed in construction stages 3 and 4. The weight of the deck was added to each individual girder using a dis-

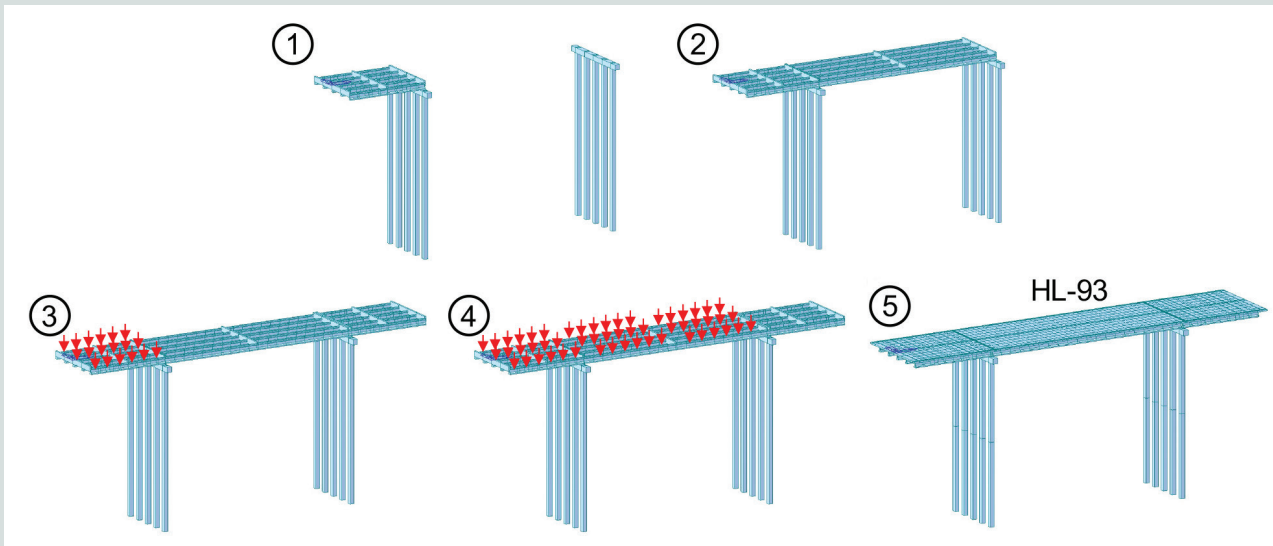


**Figure 11.** Construction stages analyzed for bridge 1. Note: Red arrows represent the dead load added to the model due to the placement of the concrete deck. HL-93 = AASHTO LRFD specifications standard live load.

tributed load with a magnitude of 0.8 kip/ft (11.7 kN/m). This distributed load was determined based on an 8 in. (200 mm) thick concrete deck, 8 ft (2.4 m) beam spacing, and normal-weight concrete (150 lb/ft<sup>3</sup> [2405 kg/m<sup>3</sup>]). Construction stage 5 was the completed structure with a standard HL-93 live load<sup>17</sup> applied. This construction stage was modeled in two ways: with a continuous deck allowing the bridge to be considered simple span for dead load and continuous for live load (SDCL) and with a joint over the supports.

**Results** We compared a fixed pile-to-cap connection and a partially fixed connection for this bridge because a pinned connection with no rotational stiffness between the pile and pile cap resulted in an unstable structure for most of the models. The behavior of the structure during construction stages 1 through 4 was not significantly affected by the type of pile-to-cap connection. The moment demand in the connections during these construction stages was also found to be relatively minor (about 10% of the full moment capacity of the 18 in. [460 mm] piles). The only requirement during these construction stages was that a sufficient moment capacity be provided to resist the moment caused by the unsymmetric placement of the support bearing on the cap.

The moment and shear demand on the superstructure in construction stage 5 were generally unaffected by the pile-to-cap connection type, but the demand on the piles was affected. There was no observed difference in moment demand on the superstructure for composite beams with a continuous deck regardless of connection type (Fig. 12), but the fixed connection generated about 43% more moment from the superstructure into the piles compared with the rotational spring connection, with maximum positive moment demands of 632 kip-in. (71.4 kN-m) for rotational spring connections and 903 kip-in. (102 kN-m) for fixed connections (Fig. 12).

The type of joint had no impact on the axial load demand in any of the piles for any of the construction stages.

## Bridge 2: Post-tensioned segmental box girder with fixed pier tables and lateral load on substructure

**Bridge description** Structures that are designed to resist large lateral loads (such as ship impact or seismic loads) are sensitive to the assumed fixity between the pile and pile cap or footing. Designs for bridges that are located over navigable waters typically must consider possible impact from vessels such as barges or ocean-going ships.<sup>1</sup>

The second bridge type analyzed was a post-tensioned segmental box-girder bridge with a fixed pier table. Several bridge configurations were analyzed with a constant depth and three spans with either equal span lengths (145 ft [44.2 m]) or span lengths associated with a balanced-cantilever approach. The balanced-cantilever spans were selected such that the outer span lengths were 60% of the main span length, resulting in span lengths of 118, 199, and 118 ft (36.0, 60.7, and 36.0 m).

Two pile cap locations were considered in this model: one with the pile cap at the water level (typical) and one with the pile cap at the soil level. The lateral load was located at the water level; therefore it was located at the pile cap when the pile cap was at the waterline. For the soil-level cap, the lateral load was located at the midheight of the pier. When the pile cap was at soil level, soil-structure interaction was applied to the entire pile (40 ft [12.2 m]) and the piers had a total height of 85 ft (25.9 m). When the pile cap was at the water level, 40 ft of the pile was embedded in soil and 15 ft (4.6 m) of the pile extended from the bottom of the pile cap

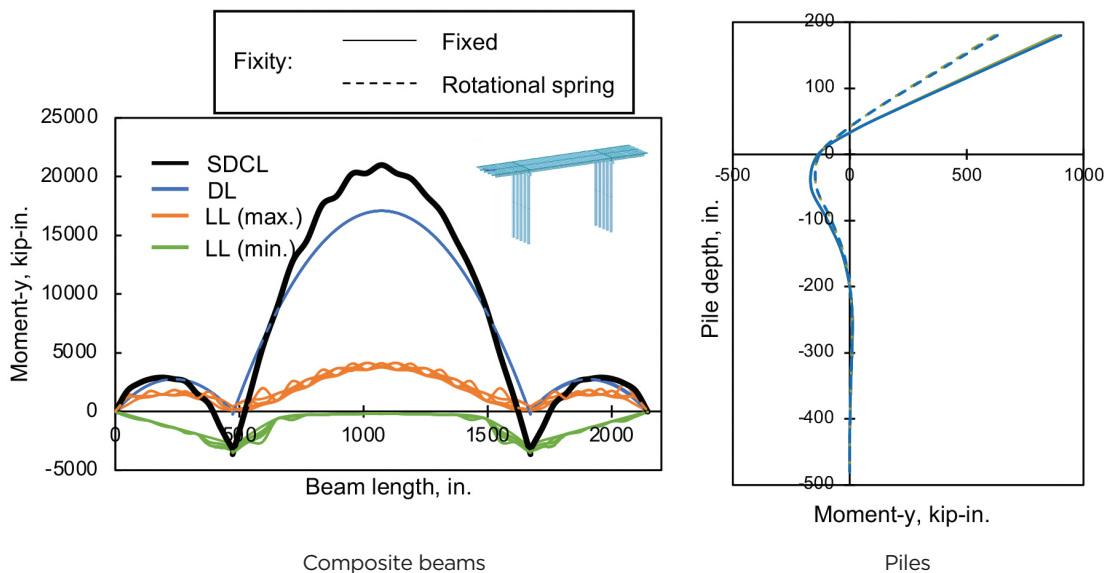


**Figure 12.** Moment demand in the composite beams and piles for bridge 1 with continuous deck in service (construction stage 5). Note: DL = dead load; LL = live load; max. = maximum; min. = minimum; SDCL = bridge considered simple span for dead load and continuous for live load. 1 in. = 25.4 mm; 1 kip-in. = 0.113 kN-m.

to the soil and did not have soil-structure interaction. The total height of the pier for the water-level pile caps was 65 ft (19.8 m).

The AASHTO-PCI-ASBI (American Segmental Bridge Institute) standard box girder 2100-1 with a deck width of 34.5 ft (10.5 m) and height of 6.9 ft (2.1 m) was selected as the cross section for this bridge. A concrete strength of 5.5 ksi (38 MPa) was used for the box girder, piers, and pile caps.

Pile designs were based on FDOT standard plans for prestressed concrete piles.<sup>16</sup> Square prestressed concrete piles with a 24 in. (610 mm) width were used for bridge 2's initial pile configuration (3 × 4–pile grid). The pile size was later increased to 30 in. (760 mm) and the pile configuration was modified to a 5 × 5–pile grid to reduce the demand on individual piles to within the capacity of the piles. The spacing of the piles was based on a minimum center-to-center spacing of  $3d_{pile}$ .<sup>1</sup> A concrete strength of 6 ksi (41 MPa) was used for the piles.

Pile cap size was based on the pile grid, with a  $3d_{pile}$  center-to-center spacing between piles and  $1d_{pile}$  space between the center of the exterior piles and the edge of the pile cap. The pile cap was 4 ft (1.2 m) thick with a concrete strength of 5.5 ksi (38 MPa). The 10 ft (3.0 m) wide piers were square, with a concrete strength of 5.5 ksi. Reinforcement was not required as an input for the pile caps or piers.

A lateral force of 2000 kip (8896 kN) was applied as a typical magnitude for vessel impact loading.<sup>1</sup> The bridge response was estimated by considering dead load, live load, and vessel impact loading using the Extreme Event II load combination from the AASHTO LRFD specifications.<sup>17</sup>

**Results** Similar results were observed for the equal-span lengths and the balanced-cantilever configuration. Results discussed in this section are only for the bridges with a 5 × 5 grid of 30 in. (760 mm) piles supporting each pier.

**Table 2** presents a summary of the maximum axial compression, axial tension, and maximum moment (absolute value) in the piles for the equal-span configuration. A similar trend was observed for the balanced-cantilever span configuration. Fixed pile-to-cap connections resulted in higher axial tension compared with pinned connections for both pile cap locations (259% increase for water-level pile caps and 23% increase for soil-level pile caps) and higher maximum moment with soil-level pile caps (240% increase). There was a slightly higher moment in the piles with pinned pile-to-cap connections and water-level pile caps compared with those with fixed connections (8% difference). There was only a small difference in the maximum axial compression based on pile-to-cap connection fixity (6% difference for water-level pile caps and less than 1% difference for soil-level pile caps).

**Figure 13** shows the moment demand in the piers for bridges with water-level and soil-level pile caps with fixed and pinned pile-to-cap connections. The moment demand on the loaded pier (pier 1) and the other pier (pier 2) are shown. The pile-to-cap connection affects the moment demand in the pier for the bridge with water-level pile caps. The moment demand in the pier increases by approximately 220% at the base of the pier and 200% at the top of the pier for pinned connections compared with fixed connections. The increased moment demand in the pier of the bridge with water-level pile caps translated to increased shear and moment demand in the superstructure caused by the lateral impact load. The moment in

the superstructure caused by the impact load increased from 105,478 kip-in. (11,917 kN-m) with fixed pile-to-cap connections to 307,786 kip-in. (34,773 kN-m) with pinned pile-to-cap connections, an increase of 192%.

The pile-to-cap connection type did not affect the behavior of the pier or the superstructure for the bridge with soil-level pile caps. The axial load in the piers was unaffected by either the type of connection between the pile and pile cap or the location of the pile cap and applied lateral load.

### Bridge 3: Straddle bent with temperature loading

**Bridge description** The third base structure that we evaluated was (6.1 m), square pier column widths of 5 ft (a straddle bent that considered temperature effects and typical dead and live loads from a post-tensioned box-girder superstructure. The base straddle bent cap had a pier height of 20 ft (1.5 m), and a bent cap beam with a length of 40 ft (12.2 m), a height of 6 ft (1.8 m), and a width of 5 ft. A moment connection was assumed between the columns and beam in the bent cap. The cross section of the beam had three rows of two 6 in. (150 mm) diameter ducts spaced at 12 in. (300 mm) apart in each direction, and each duct had twelve 0.6 in. (15.2 mm) diameter strands. The concrete strength of the columns and beam in the straddle bent was 5.5 ksi (38 MPa).

The standard 18 in. (460 mm) square piles<sup>16</sup> were modeled with 6-ksi (41 MPa) concrete. A typical 2 × 2 pile configuration

**Table 2.** Summary axial load and moment (y direction) for pile cap at water level and pile cap at soil level.

	Pile cap location			
	Water level		Soil level	
Pile-to-cap connection	Pinned	Fixed	Pinned	Fixed
Maximum axial compression, kip	325	306	493	492
Maximum axial tension, kip	22	79	103	127
Maximum moment, kip-ft	996	919	140	476

Note: 1 kip = 4.448 kN; 1 kip-ft = 1.356 kN-m.

was used with a minimum center-to-center spacing of  $3d_{pile}$  and  $1d_{pile}$  space between the center of exterior piles and edge of pile cap.<sup>1</sup> This resulted in a pile cap size of  $3d_{pile} \times 3d_{pile}$ . The thickness of the pile cap was 5 ft (1.5 m). The concrete strength for the pile caps was 5.5 ksi (38 MPa).

**Loading** We investigated two loading-related variables for bridge 3: temperature effects and superstructure loading. A uniform temperature profile and temperature gradient were both investigated, with the temperature effects considered a

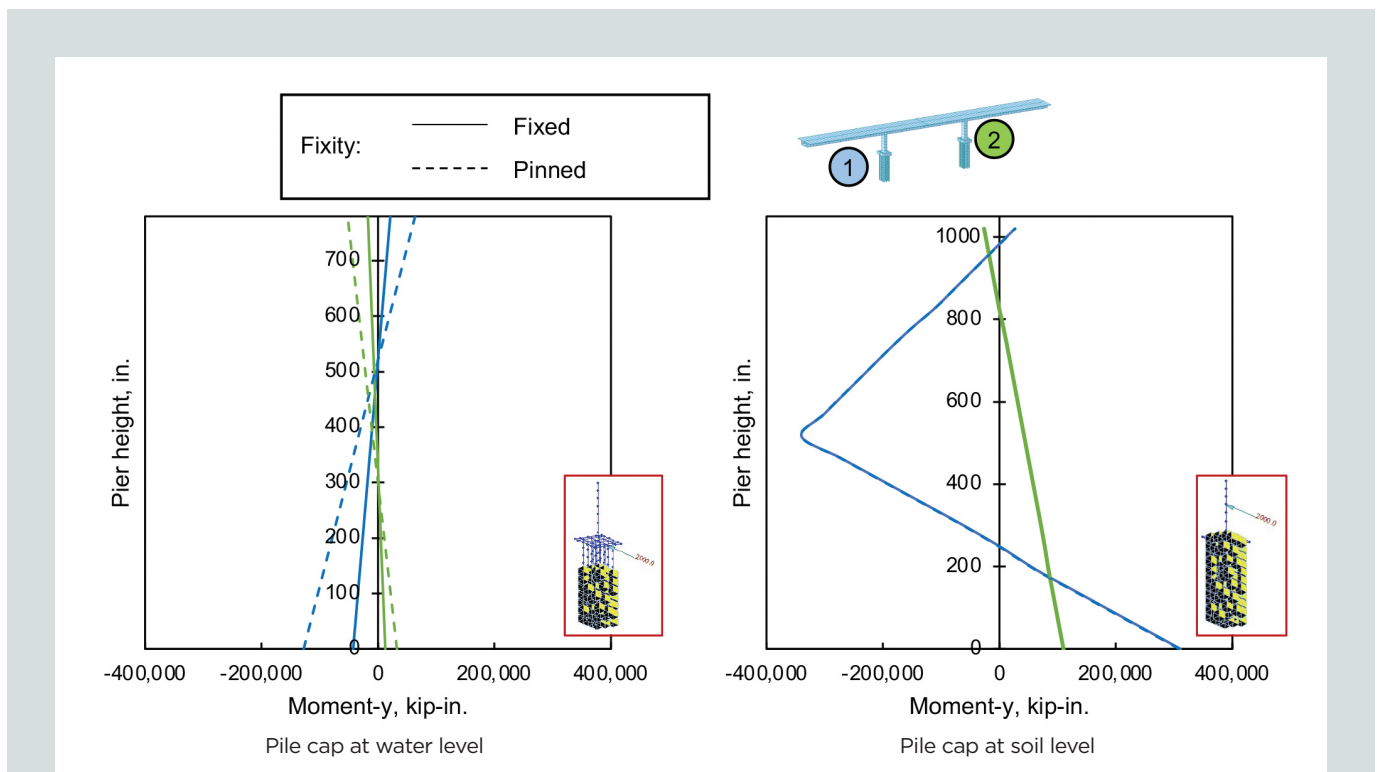


**Figure 13.** Moment (y direction) response for bridge 2 with all equal spans for laterally loaded piers. Note: The blue lines represent moment demand on the loaded pier (pier 1) and the green lines represent the moment demand on the other pier (pier 2). 1 in. = 25.4 mm; 1 kip-in. = 0.113 kN-m.

force effect due to superimposed deformation.<sup>1</sup> The temperature range selected for the uniform temperature range—35°F (1.7°C) to 105°F (40.6°C)—was based on typical values used for the design of concrete structures.<sup>1</sup> The temperature gradient was determined based on solar radiation zone 3 from the AASHTO LRFD specifications,<sup>17</sup> with a high temperature  $T_1$  of 41°F (5.0°C) and a low temperature  $T_2$  of 11°F (-11.7°C). These values were used as inputs in the Midas Civil software.

We also investigated the effect of applying a vertical load from the superstructure at the midspan of the straddle bent. This vertical load was determined from the axial load in the piers from bridge 2 (considering only dead and live loads). This factored force was 1200 kip (5340 kN). A point load was applied at midspan of the bent cap for some of the load cases to determine the system behavior considering the vertical load with uniform temperature and temperature gradient effects.

Four load cases were developed based on the possible temperature loading and vertical load:

- uniform temperature, no vertical load, post-tensioned
- uniform temperature, vertical load, post-tensioned
- temperature gradient, no vertical load, post-tensioned
- temperature gradient, vertical load, post-tensioned

The post-tensioning described previously was applied to all load cases. Long-term effects were included in the analysis by considering long-term material properties for creep and shrinkage and concrete compressive strength. The creep coefficient and shrinkage strain were automatically calculated by Midas Civil using the AASHTO LRFD specifications,<sup>17</sup> considering the volume-to-surface ratio and the compressive strength of concrete. Equation 2-1 from the American Concrete Institute's *Guide for Modeling and Calculating Shrinkage and Creep in Hardened Concrete* (ACI 209.2R-08)<sup>21</sup> was used to model the development of the concrete compressive strength over time with typical concrete compressive strength coefficients  $A$  of 4 and  $B$  of 0.85.

$$f'_c(t) = \left( \frac{t}{A + Bt} \right) f'_c$$

where

$f'_c$  = 28-day concrete compressive strength

$f'_c(t)$  = concrete compressive strength at age  $t$

$t$  = age of the concrete in days

**Results** The axial load in the piles remained in compression in all four load cases for pinned and fixed pile-to-cap connections. The axial load was not significantly affected by the fixity of the pile-to-cap connection for the cases without the vertical applied

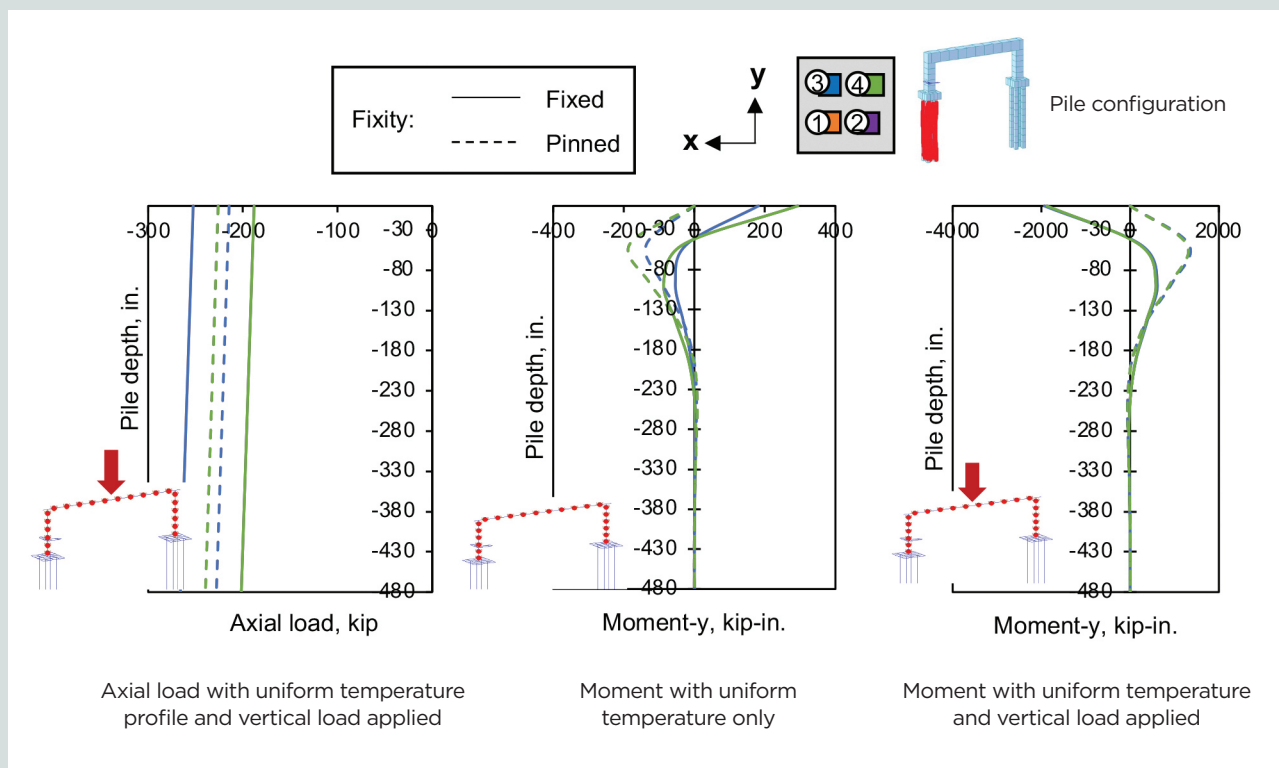


**Figure 14.** Sample pile responses for bridge 3. Note: 1 in. = 25.4 mm; 1 kip = 4.448 kN; 1 kip-in. = 0.113 kN-m.

load. The most significant difference was seen for the load cases with the vertical applied load, where the fixed connection resulted in an increased axial compression of about 10% compared with the bridge with pinned connections (Fig. 14).

The maximum moment in the piles was larger for bridges with a fixed pile-to-cap connection in all load cases (Fig. 14). The maximum moment was between 35% and 60% larger with a fixed pile-to-cap connection compared with a pinned connection.

Little to no difference in column or bent cap behavior was observed between bridges with fixed and pinned pile-to-cap connections for all four load cases (including both uniform temperature and temperature gradients).

## Bridge 4: Post-tensioned segmental box girder bridge with fixed pier table and erection mismatch

**Bridge description** The last structure that we analyzed was a segmental box-girder bridge with fixed pier tables, similar to bridge 2, except with an applied displacement in the middle of the span to simulate erection tolerances at the closure pour between the cantilevered spans (Fig. 9). The difference in elevation at this point is typically accommodated by using a steel strongback system with jacks to force the tips of the two cantilevered spans to align. Then the closure pour is cast, the continuity tendons are tensioned along the top and bottom of the section, and the strongback is released, which locks in the stresses in the structure. These locked-in stresses must be considered in the superstructure and substructure designs, and the assumed fixity of the pile-to-cap connection affects how these stresses are managed.

The base structure was the same as the one used for bridge 2 with a balanced-cantilever configuration and pile caps at soil level. Variables and parameters used in this model are presented in previous sections of this paper.

We used a typical erection tolerance for cantilever bridges with fixed pier tables of  $L_c/1000$ , where  $L_c$  is the cantilever length from the center of the pier to the cantilever tip.<sup>1</sup> For a main span of 199 ft (60.7 m), which corresponds to the main span length of the balanced-cantilever configuration, the cantilever length is 99.5 ft (30.3 m) and the corresponding tolerance is 1.19 in. (30.2 mm). Half of the structure was modeled with this applied displacement of 1.19 in. at the end of the cantilever tip.

Three common configurations of pile grids were investigated for bridge 4:

- 3 × 4 grid of 18 in. (460 mm) piles
- 2 × 4 grid of 24 in. (610 mm) piles
- 2 × 3 grid of 30 in. (760 mm) piles

The structure was modeled so that the beam was continuous over the interior pier, and a pinned support was applied at the opposite end of the structure to simulate the abutment.

**Results** There was no significant difference in axial load in the piles between bridges with fixed pile-to-cap connections and those with pinned connections for any of the pile configurations (Fig. 15). There was no moment in the piles from the forced displacement with pinned pile-to-cap connections. Only a small moment in the piles from the forced displacement was observed in the structure with fixed pile-to-cap connections (Fig. 15). These effects should be included when designing this type of structure.

There was little to no difference in the behavior of the box girder or pier based on whether a pinned or fixed pile-to-cap connection was used.

## Conclusion

We conducted a set of numerical studies using finite element analysis at two different scales to investigate the behavior of pile-to-cap connections with typical configurations at the individual member scale, and the influence of the assumed pile-to-cap connection on the behavior of the entire bridge structure for structure types that are typically assumed to be sensitive to the connection type.

To investigate the effect of pile size, pile embedment length, pile strand layout, axial load in pile, pile concrete strength, pile cap concrete strength, pile cap size, and pile cap reinforcement configuration on the connection behavior, 131 different pile-to-cap connection models were analyzed. The following conclusions can be made based on these analyses:

- Moment capacity of the pile-to-cap connection seemed to be proportional to the embedment length of the connection until the capacity of the pile was reached.
- Shallow pile embedment lengths developed significant moment; therefore, it is unlikely that a shallow embedment would provide an actual pin connection. Interface reinforcement between the pile and pile cap caused shorter embedment lengths to develop higher moments than those without interface reinforcement.
- Normalized moment response was nearly identical for normalized embedment length regardless of the considered pile sizes (18, 24, and 30 in. [460, 610, and 760 mm] piles).
- Additional axial compression applied to the pile improved the performance of the connection and increased the moment capacity in the pile.
- Pile concrete strength did not affect the performance of the connections with shallow pile embedment lengths but slightly increased the capacity of the pile-to-cap connection.

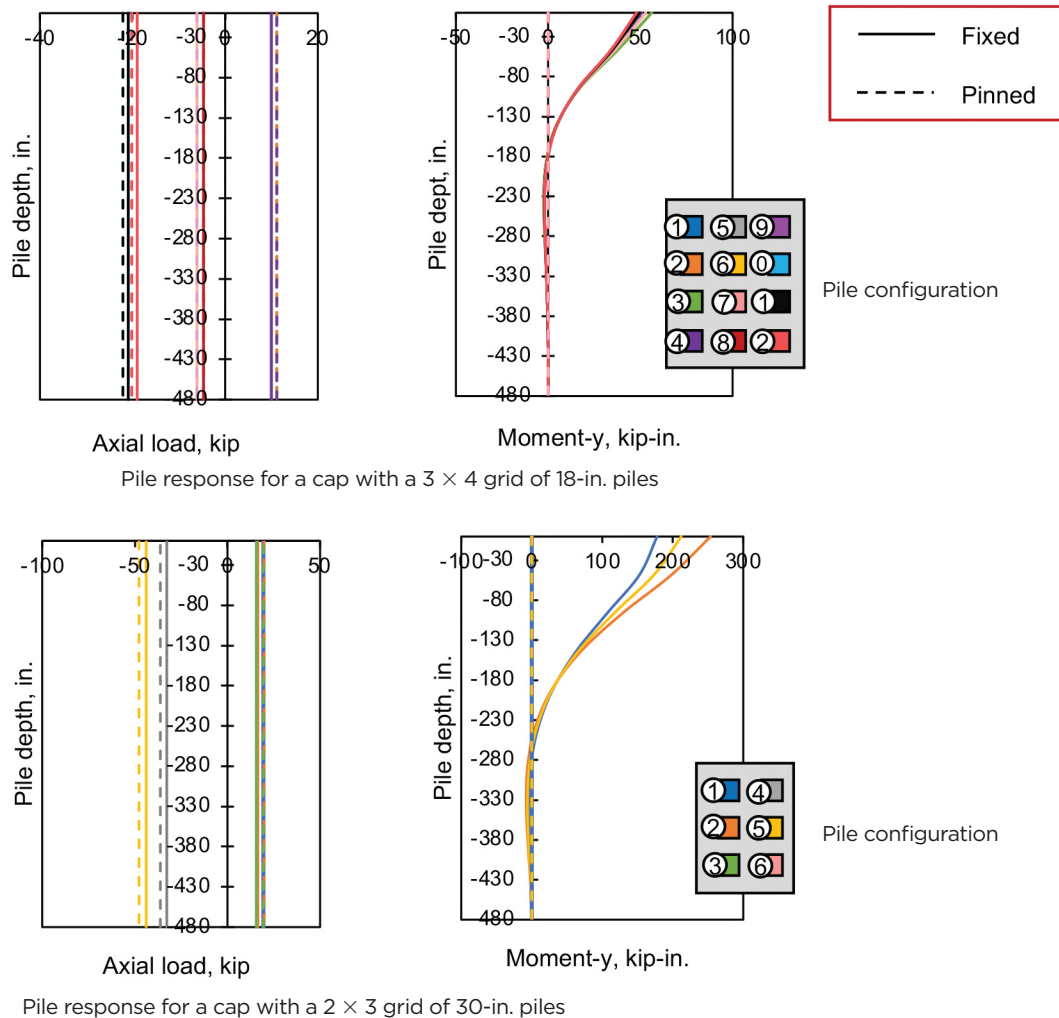


**Figure 15.** Axial load and moment response for selected piles in bridge 4. Note: 1 in. = 25.4 mm; 1 kip = 4.448 kN; 1 kip-in. = 0.113 kN-m.

tion for piles with deep embedment lengths for the range of considered concrete strengths.

- Pile cap concrete strength affected the performance of the pile-to-cap connection with shallow pile embedment; concrete crushing in the pile cap adjacent to the embedded pile controlled failure.
- The size of the pile cap did not seem to have a significant effect on the performance of the pile-to-cap connection for the range of considered pile cap sizes. Confinement reinforcement around the pile also did not have a significant effect. The shallow pile embedment with the minimum edge distance of 9 in. (230 mm) led to lower strength of the connection.
- There was little observed difference in the connection performance for piles with 0.5 in. (12.7 mm) diameter prestressing strands and those with 0.6 in. (15.2 mm)

diameter prestressing strands. The development length observed from the numerical analysis results was significantly shorter than would be estimated using AASHTO LRFD specifications.<sup>17</sup>

An experimental testing program on full-scale specimens is planned to validate these observations from the numerical studies.

Four base structures considered to be sensitive to the pile-to-cap connection fixity and with several different variations of each structure were analyzed to determine the effect of the assumed pile-to-cap connection on the overall behavior of the entire bridge structure. The following conclusions can be made based on these models:

- Bridge 1, simple spans with uneven span lengths: When a pinned connection was assumed for bridges where the structure was unstable in the construction stage, the

connection did not significantly affect the behavior of the final structure. However, sufficient embedment length should be provided to resist moments caused by eccentrically placed up-station and down-station girders.

- Bridge 2, post-tensioned segmental box-girder bridge with fixed pier tables and lateral load on substructure: The location of the pile cap (water level or soil level) changed the way the pile-to-cap connection fixity affected the behavior of the bridge. Piles with pinned connections in water-level pile caps saw increased moment (8%) compared with fixed connections in water-level pile caps, whereas piles with fixed connections in soil-level pile caps saw a larger moment increase (240% greater) compared with pinned connections in soil-level pile caps. The moment demand in the piers of bridges with water-level pile caps was 220% greater at the base of the pier and 200% greater at the top of the pier for pinned pile-to-cap connections (compared with fixed connections), which translated to a greater demand on the superstructure. The pile-to-cap connection type did not affect the behavior of the pier or the superstructure for the bridge with soil-level pile caps. The axial load in the piers was unaffected by either the type of pile-to-cap connection or the location of pile cap and applied lateral load.
- Bridge 3, straddle bent with temperature loading: The maximum moment in the piles was 35% to 60% greater for bridges with a fixed pile-to-cap connection compared with bridges using pinned pile-to-cap connections in all load cases. Little to no difference in behavior was observed in the columns or bents.
- Bridge 4, post-tensioned segmental box-girder bridge with fixed pier table and erection mismatch: The forced alignment of the cantilevers led to additional moment in the piles with a fixed pile-to-cap connection and no additional moment for piles with pinned connections. There was no other significant difference in behavior based on connection type.

This paper demonstrates that the pile-to-cap connection can significantly influence the behavior of bridge structures. Understanding whether the connection exhibits pinned or fixed behavior may result in better design guidelines for future structures.

## Acknowledgments

The research presented in this project was supported by the Florida Department of Transportation (FDOT). The authors would like to thank FDOT for its financial support, Christina Freeman for her guidance on the project, and the team of engineers at FDOT for their careful review of the research results. The opinions, findings, and conclusions expressed in this publication are those of the authors and not necessarily those of FDOT or the U.S. Department of Transportation.

## References

1. FDOT (Florida Department of Transportation). 2021. *FDOT Structures Design Guidelines—Structures Manual*, vol. 1. Tallahassee, FL: FDOT. <https://www.fdot.gov/structures/docsandpubs.shtm>.
2. MnDOT (Minnesota Department of Transportation). 2019. "Section 10: Foundations." In *LRFD Bridge Design*. St. Paul, MN: MnDOT.
3. WisDOT (Wisconsin Department of Transportation). 2021 "Chapter 11: Foundation Support." In *WisDOT Bridge Manual*. Madison, WI: WisDOT.
4. CDOT (Colorado Department of Transportation). 2018. *CDOT LRFD Bridge Design Manual*. Denver, CO: CDOT.
5. IDOT (Illinois Department of Transportation). 2012. *Bridge Manual*. Springfield, IL: IDOT. <https://idot.illinois.gov/Assets/uploads/files/Doing-Business/Manuals-Guides-&-Handbooks/Highways/Bridges/Bridge%20Manual%202012.pdf>.
6. NHDOT (New Hampshire Department of Transportation). 2015. "Chapter 6: Substructure." In *Bridge Design Manual*. Concord, NH: NHDOT. <https://www.nh.gov/dot/org/projectdevelopment/bridgedesign/manual.htm>.
7. ODOT (Oregon Department of Transportation). 2020. *Bridge Design Manual*. Salem, OR: ODOT.
8. Harries, K., and M. Petrou. 2001. "Behavior of Precast, Prestressed Concrete Pile to Cast-in-Place Pile Cap Connections." *PCI Journal* 46 (4): 82–92. <https://doi.org/10.15554/pcij.07012001.82.92>.
9. Rollins, K. M., and T. E. Stenlund. 2010. *Laterally Loaded Pile Cap Connections*. UT-10.16. Salt Lake City, UT: Utah Department of Transportation. <https://rosap.nrl.bts.gov/view/dot/18449>.
10. Xiao, Y. 2003. "Experimental Studies on Precast Prestressed Concrete Pile to CIP Concrete Pile-Cap Connections." *PCI Journal* 48 (6): 82–91. <https://doi.org/10.15554/pcij.11012003.82.91>.
11. Xiao, Y., H. Wu, T. T. Yaprak, G. R. Martin, and J. B. Mander. 2006. "Experimental Studies on Seismic Behavior of Steel Pile-to-Pile-Cap Connections." *Journal of Bridge Engineering* 11 (2): 151–159. [https://doi.org/10.1061/\(ASCE\)1084-0702\(2006\)11:2\(151\)](https://doi.org/10.1061/(ASCE)1084-0702(2006)11:2(151)).
12. Shama, A. A., J. B. Mander, and A. J. Aref. 2002. "Seismic Performance and Retrofit of Steel Pile to Concrete Cap Connections." *ACI Structural Journal* 99 (1): 51–61. <https://doi.org/10.14359/11035>.

13. ElBatanouny, M. K., P. Ziehl, A. Larosche, T. Mays, and J. Calcedo. 2012. "Bent-Cap Confining Stress Effect on Slip of Prestressing Strands." *ACI Structural Journal* 109 (4): 487–496. <https://doi.org/10.14359/51683868>.
14. Issa, M. 1999. *Testing of Pile-to-Pile Cap Moment Connection for 30" Prestressed Concrete Pipe-Pile*. Report 98-9. Tallahassee, FL: FDOT.
15. Ramberg, W., and W. R. Osgood. 1943. "Description of Stress-Strain Curves by Three Parameters." Technical Note 902. Washington, DC: National Advisory Committee for Aeronautics.
16. FDOT. 2019. *Prestressed Concrete Piles: Standard Plans*. Index 455–400 and 455–440. Tallahassee, FL: FDOT. <https://www.fdot.gov/design/standardplans/2020>.
17. AASHTO (American Association of State Highway and Transportation Officials). 2017. *AASHTO LRFDF Bridge Design Specifications*. 8th ed. Washington, DC: AASHTO.
18. Larosche, A., P. Ziehl, M. ElBatanouny, and J. Caicedo. 2014. "Plain Pile Embedment for Exterior Bent Cap Connections in Seismic Regions." *Journal of Bridge Engineering* 19 (4): 1–12. [https://doi.org/10.1061/\(ASCE\)BE.1943-5592.0000542](https://doi.org/10.1061/(ASCE)BE.1943-5592.0000542).
19. Shahawy, M., and M. Issa. 1992. "Effect of Pile Embedment on the Development Length of Prestressing Strands." *PCI Journal* 37 (6): 44–59. <https://doi.org/10.15554/pcij.11011992.44.59>.
20. PCI. 2010. *PCI Design Handbook*. 7th ed. Chicago, IL: PCI.
21. American Concrete Institute (ACI) Committee 209. 2008. *Guide for Modeling and Calculating Shrinkage and Creep in Hardened Concrete*. ACI 209.2R-08. Farmington Hills, MI: ACI.
- $f_{p2}$  = second critical strength for prestressing steel
- $f_{p3}$  = ultimate strength for prestressing steel
- $f'_c$  = 28-day concrete compressive strength
- $f'_c(t)$  = concrete compressive strength at age  $t$
- $H$  = height of the pile cap specimen
- $k$  = spring rotational stiffness for pile-to-cap connection
- $K_x$  = modulus of subgrade reaction in the x direction
- $K_y$  = modulus of subgrade reaction in the y direction
- $L$  = length of the pile cap specimen
- $L_c$  = the cantilever length from the center of the pier to the cantilever tip
- $t$  = age of the concrete in days
- $T_1$  = high temperature value of temperature gradient
- $T_2$  = low temperature value of temperature gradient
- $W$  = width of the pile cap specimen
- $\epsilon_1$  = yield strain for mild reinforcement
- $\epsilon_2$  = ultimate strain for mild reinforcement
- $\epsilon_{p1}$  = yield strain for prestressing steel
- $\epsilon_{p2}$  = second critical strain for prestressing steel
- $\epsilon_{p3}$  = ultimate strain for prestressing steel

## Notation

- $A$  = concrete compressive strength coefficient
- $A_g$  = gross area of concrete pile section
- $B$  = concrete compressive strength coefficient
- $d_{pile}$  = depth of pile
- $f_1$  = yield strength for mild reinforcement
- $f_2$  = ultimate strength for mild reinforcement
- $f_{p1}$  = yield strength for prestressing steel

## About the authors



Isabella Zapata is a PhD student in the Department of Civil and Environmental Engineering at Florida International University in Miami. She received her BS from Pontificia Universidad Javeriana Cali in Colombia, and her MS from Florida International University.



John Corven, PE, is director of complex bridges for Corven Engineering/Hardesty & Hanover in Tallahassee, Fla. He has been designing and participating in the construction engineering of complex concrete bridges for 41 years. He received his BSCE and ME from the University of Florida.



Seung Jae Lee, PhD, is an associate professor in the Department of Civil and Environmental Engineering at Florida International University. He received his BS from Sungkyunkwan University in Korea and both his MS and PhD from the University of Illinois at Urbana-Champaign.



David B. Garber, PhD, PE, is an associate professor in the Department of Civil and Environmental Engineering at Florida International University. He received his BS from Johns Hopkins University in Baltimore, Md., and both his MS and PhD from the University of Texas at Austin.

## Abstract

This paper presents the results of analytical studies on the connection between piles and pile caps or footings. Two nonlinear finite element analysis software packages were used to investigate the behavior of the connection itself and the impact of connection assumptions on the overall behavior of different sensitive structures such as simple spans with uneven span lengths, segmental box girders with fixed pier tables, and straddle bents with temperature loading. Results show that the behavior of the connection is affected by variables such as pile size, pile embedment length, pile cap concrete strength, interface reinforcement, and distance between the edge of the pile and the edge of the pile cap. The study also demonstrated that significant moment can develop even with shallow pile embedment lengths. The assumed level of fixity between the pile and pile cap was found to significantly influence the behavior of some of the bridges investigated in this study.

<https://doi.org/10.15554/pcij67.1-01>

## Keywords

Pile embedment length, pile-to-cap connection, segmental box girder with fixed pier table, sensitive structures, straddle bent with temperature loading.

## Review policy

This paper was reviewed in accordance with the Precast/Prestressed Concrete Institute's peer-review process.

## Reader comments

Please address any reader comments to *PCI Journal* editor-in-chief Tom Klemens at [tklemens@pci.org](mailto:tklemens@pci.org) or Precast/Prestressed Concrete Institute, c/o *PCI Journal*, 8770 W. Bryn Mawr Ave., Suite 1150, Chicago, IL 60631. [f](#)